Numbers of Scaled and Matched Accelerograms Required for Inelastic Dynamic Analyses

Jonathan Hancock, Julian J. Bommer and Peter J. Stafford[1]
Department of Civil & Environmental Engineering, Imperial College London, SW7 2AZ, UK

SUMMARY

Selecting, scaling and matching accelerograms is critically important to engineering design and assessment, enabling structural response to be determined with greater confidence and through fewer analyses than if unscaled accelerograms are employed. This paper considers the response of an 8-storey MDOF reinforced concrete structure to accelerograms selected, linearly scaled or spectrally matched using five different techniques. The first method consists of selecting real records on the basis seismological characteristics, while the remaining methods make an initial selection on the basis of magnitude and spectral shape before: (1) scaling to the target spectral acceleration at the initial period; (2) scaling to match the target spectrum over a range of periods; (3) using wavelet adjustments to match the target spectrum; and (4) using wavelet adjustments to match multiple target spectra for different damping ratios. The analyses indicate that the number of records required to obtain a stable estimate of the response decreases drastically as one moves through these methods. The exact number varies among damage measures and is shown to be related to the predictability of the response measure that is considered. For measures such as peak roof and inter-storey drift, member end-rotation and Park and Ang damage, as few as one or two records are required to estimate the response to within ±5% (for a 64% confidence level) if matching to multiple damping ratios is conducted. Bias checks are made using predictive equations of the expected response derived from the results of 1656 non-linear time-domain analyses of the structure under the action of unscaled accelerograms.

Keywords: inelastic demand; damage potential; accelerogram selection; accelerogram scaling; accelerogram matching.

1. INTRODUCTION

In order to carry out inelastic dynamic analysis structural engineers require a suite of accelerograms that are consistent with some predefined earthquake scenario, often obtained from a probabilistic seismic hazard analysis (PSHA). Each record that is consistent with this scenario will affect the structure in a different way and the value of a chosen damage measure given this scenario will therefore vary. The objective of selecting and scaling accelerograms is to obtain a suite of ground motions that induce the same inelastic response as the either the mean inelastic response, or some target percentile response, that would be found if the structure were to be analysed with a large suite of ground motions consistent with the design scenario. This design scenario typically consists of a magnitude, source-to-site distance and site classification as well as other parameters in some cases.

---

[1] Corresponding author: T: +44-20-7594-6030, F: +44-20-7594-5934, E: p.stafford@imperial.ac.uk

The purpose of this paper is to investigate various options for scaling and matching accelerograms in order to identify efficient methods for obtaining the expected inelastic response of a structure as assessed by some damage measure. The efficiency here relates directly to the number of records that are required in order to obtain an accurate representation of the expected response and this is therefore the metric by which the various methods are judged.

Currently, the minimum number of records required to be used in inelastic dynamic analysis by design codes varies but is frequently based (e.g. IBC 2000; Bommer and Ruggeri 2002; CEN 2004) upon the guidance of the 1994 Uniform Building Code (UBC 1994). This document states that the maximum response should be used if three records are used, while the average response may be used if seven or more records are used. However, the code drafting committee made this recommendation based on what they considered to be a "reasonable" number of analyses within a design office environment and it has no scientific basis (Kircher 2005). The key issue addressed in this paper is how many records are required to obtain a stable and unbiased estimate of the inelastic response of a structure. Shome *et al.* (1998) point out that the number of records required to obtain an estimate of the median response to within a defined confidence interval depends on the standard deviation of the response. Therefore the number of records to be used should depend on both the procedure used to select and scale the accelerograms and the nature of the structural response being investigated. Shome *et al.* (1998) also found that linearly scaling accelerograms to the initial period of the structure could reduce the number of runs required to estimate the median response by a factor of about four, compared to using unscaled records from a magnitude and distance bin centred on the design scenario. These findings are further investigated in this study.

Studies by other authors using accelerograms adjusted to match a target response spectrum produce conflicting conclusions. The study of Naeim and Lew (1995) uses a frequency domain adjustment to create spectrally matched accelerograms. They find that the maximum building displacement under the matched accelerograms is approximately twice that under the action of accelerograms linearly scaled to exceed the target spectrum. This is probably because the procedure used to adjust these accelerograms creates a base-line drift in the displacement time-series of the ground motion and also introduces high levels of energy into the accelerograms. Carballo (2000) found that using spectrally matched accelerograms led to an underestimation of the response. The work described in this paper investigates if either of these apparently contradictory findings is applicable to accelerograms adjusted using the latest version of RspMatch (Hancock *et al.* 2006). Carballo (2000) also found that matching accelerograms to a target spectrum reduced the number of accelerograms required to achieve an estimate of the median response to within a given confidence level by a further factor of about four compared to using accelerograms linearly scaled to the spectral acceleration of the target spectrum at initial period of the structure. This study also investigates this finding using the latest version of RspMatch.

Over recent years the complexity of procedures for selecting, scaling and matching accelerograms has increased (*e.g.*, Lee *et al.* 2000; Malhotra 2003; Naeim *et al.* 2004; Baker and Cornell 2006; Watson-Lamprey and Abrahamson 2006a; and Zhai and Xie 2007) and these issues continue to be topics of active research. However, it is likely to be sometime before such state-of-the-art methods are disseminated into common practice. This study therefore presents the results of analyses that are broadly based upon the comparatively simple selection criteria proposed by Bommer and Acevedo (2004) that may be regarded as reflecting the current state-of-practice. The expected inelastic response, as estimated using a variety of damage measures, of a seismically designed 8-storey MDOF reinforced concrete wall-frame structure is determined by conducting regression analyses on the response of the structure under the action of 1656 unscaled accelerograms. This regression analysis allows for the distribution of the various considered damage measures to be estimated. Five different scaling or matching procedures are then applied to suites of records and the associated inelastic response is compared with the expected values from the regression analysis to check for bias and to determine the number of accelerograms required to predict the expected response to within a specified interval at a given confidence level.

2. MODELS AND ANALYSIS

2.1 Structural model

The structural model used in this study has been described extensively by Hancock and Bommer (2007). The structure, shown schematically in Figure 1, is an 8-storey regular wall-frame reinforced concrete building designed to Eurocode 8 (CEN 2004). The structure has been designed with a medium ductility classification, a behaviour factor of 2.625 and a design PGA of 0.15g. All structural analyses are performed using the finite element program SeismoStruct (SeismoSoft 2005).

2.2 Ground-motion dataset

The accelerograms used in this study are taken from the PEER NGA database (PEER 2006). Records are only used if the moment magnitude, site classification and source-to-site distance are known. Records from Taiwan are excluded to reduce the size of the database and to prevent the 1813 accelerograms from the Chi-Chi earthquake sequence dominating the results. Records where either component has a high-pass filter frequency greater than 0.33Hz (less than 3s period) have also been excluded. The magnitude-distance distribution of the dataset is given in Figure 2. The site classification is based on the average shear-wave velocity over the upper 30m (V_{s30}) and the records are grouped into three categories according to their V_{s30} value. The grouping follows Boore and Joyner (1993) and Ambraseys *et al.* (1996) as follows: sites with $V_{s30} > 760$m/s are classed as rock; sites with V_{s30} between 360m/s and 760m/s are classed as stiff soil; and those with a V_{s30} less than 360m/s are classified as soft soil. The style-of-faulting used herein follows the classifications given in the NGA dataset and are determined using an estimate of the rake angle of the earthquake (PEER 2006). Residuals from predictive equations developed in this work show that earthquakes with reverse-oblique mechanism have similar trends to those from reverse faulting events and these two classes are therefore combined.

2.3 Damage measures

A large number of damage measures are proposed in the literature for reinforced concrete structures. However, these may be generically grouped into four main categories:

1. Measures of maximum response (force or displacement);
2. Cyclic fatigue measures;
3. Energy measures;
4. Measures using a combination of the above.

No attempt is made herein to consider all of the proposed damage measures but rather a set of six commonly used and representative measures are selected that include at least one measure from each of the above groups. These damage measures are:

- Peak roof drift (maximum response);
- Peak inter-storey drift, for all storeys (maximum response);
- Peak member end rotation, local member damage measure (maximum response);
- Member rotational fatigue, local member damage measure (fatigue measure);
- Absorbed hysteretic energy, local member damage measure (energy measure);
- Park and Ang (1985) damage index, local member damage measure (combination measure).

While these damage measures will be familiar to many readers, a comprehensive description of each of them has recently been provided by Hancock and Bommer (2007) and interested readers are referred there for further details. For the damage measures that require parameters to be assumed or defined, such as the member rotational fatigue damage measure, the values used by, and detailed in, Hancock and Bommer (2007) are retained for this study.

2.4 Definition of the 'average' response

Most design codes require accelerograms to be scaled so that the average of their response spectra matches or exceeds the target spectrum. Many codes also then permit the average structural response to be taken. However, the term 'average' is somewhat ambiguous as there are numerous mathematical measures of the central tendency of a data set that may all be loosely referred to as the average. In earthquake engineering three such measures commonly arise: the arithmetic mean, the geometric mean, and the median. From presentations by and discussions with the US code drafters (e.g., Kircher 2005) it is clear that they intended the arithmetic mean to be used when developing the code provisions; the arithmetic mean is also specified by Eurocode 8 (CEN 2004). However, empirical ground-motion models that are used to derive target spectra assume the ground motions to be log-normally distributed and the use of the geometric mean of the accelerograms is therefore more consistent with the specification of the target spectra (note that although the geometric mean and the median are the same for the log-normal distribution, this is generally not true for a sample from this distribution and the geometric mean is therefore preferred over the median due to its greater stability). Likewise, it is common to assume that the measure of structural response is log-normally distributed (e.g., Cornell *et al.* 2002) and it is therefore most appropriate to represent the 'average' structural response by the geometric mean. However, the consequence of this issue is not great if a consistent definition is used for both scaling the accelerograms and for measuring the response. Essentially, using the arithmetic mean rather than the geometric mean decreases the applied loading but simultaneously increases the estimate of the observed response and one obtains a similar estimate of the response to that obtained through consistently using the geometric mean. The similarity between the two approaches is related to the relative standard deviations (dispersions) of the log-normal distributions of the ground motions and the response. Regardless, the geometric mean of the selected, scaled and matched spectra is adopted for the current work.

2.5 Estimating the expected PSA and damage from unscaled records

Every accelerogram that is passed through a structure will induce a different level of response. This response, as measured by any of a number of damage measures, may therefore be modelled as a distribution, the most common of which is the log-normal distribution. The dispersion of this distribution is directly related to the number of records required to obtain a stable estimate of the inelastic response (Shome *et al.* 1998). In order to obtain estimates of the distributions of the considered responses for a particular earthquake scenario one may select a large suite of accelerograms that are consistent with this scenario and fit a distribution to the responses that are observed upon passing these accelerograms through a structure. However, for many earthquake scenarios of engineering interest there will be a relatively small number of records available and the distribution thus obtained may not truly reflect the expected inelastic response under the actions imposed by future earthquakes. An alternative approach is to use a very large number of accelerograms from a broad range of magnitudes, distances and site classes in order to develop empirical predictive equations for various damage measures. In this approach, although the number of records that are available for a particular scenario does not change, a great deal of additional constraint on the expected inelastic response is provided by the records from other magnitudes and distance ranges. The distributions of damage measures are therefore less likely to be biased through peculiarities of a particular suite of accelerograms when regression analyses are conducted.

In this study, regression analysis is used to derive predictive equations for pseudo spectral acceleration (PSA) and for the different damage measures listed in section 2.3. The one-stage maximum likelihood regression method of Joyner and Boore (1993) is used in an attempt to remove biases associated with the correlation of ground motions within individual earthquakes. In order to simplify the regression analyses, the same functional form was used for the equations of spectral acceleration and for all of the damage measures and is given in Equation (1).

$$\log_{10}(y) = c_1 + c_2 M_w + c_3 M_w^2 + c_4 \log_{10}\left(\sqrt{R_{jb}^2 + c_6^2}\right) + c_5\sqrt{R_{jb}^2 + c_6^2} + c_7 S_1 + c_8 S_2 + c_9 F_1 + c_{10} F_2 \quad (1)$$

Here $\log_{10}(y)$ is the logarithm of the parameter to be regressed; $c_{1,\ldots,10}$ are the model coefficients to be determined through the regression; M_w is moment magnitude; R_{jb} is the closest distance to the surface projection of the fault rupture, as proposed by Joyner and Boore (1981); S_1 and S_2 are dummy variables that have values of one for soft soil and stiff soil sites respectively and values of zero otherwise; F_1 and F_2 are similar dummy variables for style-of-faulting that have values of one for normal and reverse or reverse-oblique faulting earthquakes and zero otherwise. The total standard deviation, σ_T, of the model in Equation (1) is comprised of two independent components, the intra-event variability, σ_A, and the inter-event variability, σ_E:

$$\sigma_T = \sqrt{\sigma_E^2 + \sigma_A^2} \quad (2)$$

This functional form and variance structure has successfully been used to model peak ground acceleration and spectral accelerations in the past and many of the considered damage measures tend to scale in a similar manner with respect to common predictor variables, both in terms of their median response and their associated distributions. Details of the exploration of functional forms as well as residual plots for all of the considered damage measures may be found in Hancock (2006). Clearly, the use of different functional forms for different damage measures and for different positions within the structure (i.e., one functional form for seventh-storey drift and another for first-storey drift) may result in better constraints on the distributions of damage measures. However, for any realistic structure, the effort required to derive structure-specific predictive models for the very large number of combinations of damage measure and structural position is untowardly onerous. For this reason we have adopted the ten parameter functional form in Equation (1) for all situations. In some cases this approach will lead to an over-parameterised model but as the purpose of the analysis is to derive models for this particular set of ground-motions and this specific structure, issues associated with over-parameterisation are not important. Examples of the general scaling of the predictive equations with respect to magnitude and distance are shown in Figure 3. When examining these predictions it should be borne in mind that large drifts are not to be expected as this is a stiff wall-frame structure that has been designed for seismic resistance.

While the two-dimensional wall-frame model used in this study can accurately model global parameters, such as inter-storey drift, local effects are less accurately modelled. For example, greater deformations, damage and inelasticity would be expected in the beams of the outer frames of the structure than is indicated from the single-frame model (Mwafy 2001). For this reason, the absolute values of the local damage measures have little meaning. However, as the MDOF model is consistent among all of the analyses, these measures can still be used to quantify the ability of different methods of selecting, scaling and matching accelerograms to efficiently estimate different types of local damage measures.

The standard deviations provided for each of the damage measures in Figure 3 show that the member rotational fatigue has the greatest variance of all of the damage measures and is one of the most difficult to predict with empirical equations. The analyses, detailed in Hancock (2006), indicate that the predictive equation for rotational fatigue may over-estimate the damage in the members for earthquakes with magnitudes over M_w 6.0 and source-to-site distances less than 30km. There is also a significant variability associated with the prediction of hysteretic energy. As is shown in section 4, the larger the variance in the damage measure, the greater the number of records that are required to obtain a robust estimate of the structural response. The numbers of records required to predict the peak and combination measures considered in this study are significantly less than the energy- and fatigue-based measures.

Several scaling methods require estimates of the elastic spectral acceleration at a single period or over a range of periods. Although many equations have previously been derived for this purpose (e.g., Douglas 2003) it is preferable to develop a suite of equations that are internally consistent, in terms of having been derived from the same dataset, for both the specification of the spectral accelerations and the estimates of the inelastic response. A set of predictive equations is therefore derived for pseudo spectral acceleration at damping ratios of 1, 5, 10 and 20% for use with the scaling and matching techniques described in the following section. Coefficients of the new equations are not presented here as they have not been derived for general use, however they may be found in Hancock (2006). Although the new equations generally exhibit the same trends as other previously derived equations, there are significant differences in the predictions; thus highlighting the range of predictions that may be obtained through the use of different datasets, functional forms and regression techniques. The existence of such differences demonstrates the importance of deriving a suite of internally consistent predictive equations, as has been done in this study.

3. SELECTION AND SCALING OF RECORDS

3.1 Target scenario and record selection

The structure used in this investigation has been designed to resist seismic actions in accordance with a modern design code and so genuinely ‘strong’ ground-motions are required to induce inelastic response. The target scenario used for this work is an M_w 7.0 strike-slip earthquake at 5km distance from a site with soft soil conditions. Both the median and 84th-percentile target spectra are used as this allows two levels of loading to be investigated. The use of the 84th percentile spectra also investigates the assumption, commonly made in practice, that structural response under the action of an accelerogram scaled or adjusted to match an 84th percentile ground motion will produce an 84th percentile response. The purpose of analysing the structural response under the actions of accelerograms scaled to 84th percentile spectral levels is to explicitly demonstrate the flaw in this assumption.. Although in this study a hypothetical scenario is selected, in practice the design scenario may be derived from either disaggregating a hazard curve from a PSHA (e.g., McGuire 1995) or by conducting a deterministic seismic hazard assessment. The vertical component of the ground motion is not used in this study to ensure that the characteristics of the observed response are only caused by the horizontal component of the ground motion.

Nine groups of 25 records are selected for scaling and matching using the different methods outlined in Table 1. The first group of records (group A) consists of unscaled accelerograms chosen to match the seismological characteristics of the scenario event These records are recorded from earthquakes within ±0.2 magnitude units of the scenario event with soft or stiff soil site classification and are located within 10.5 km of the surface projection of the fault rupture (i.e., $R_{jb} < 10.5$ km). Only the larger component, selected from the elastic spectral acceleration at the initial period of the structure (0.56s), is used from each record. The spectral characteristics of the records are shown in Figure 4. This figure indicates that on average the 5% damped elastic response spectra of these records have a good match to both the median and 84th-percentile target spectra over the period range of greatest relevance to this structure (0.25s to 1.25s).

Records for the remaining groups (B1, B2, C1, C2, D1, D2, E1 and E2) are selected using the methodology proposed by Bommer and Acevedo (2004). These records are chosen from earthquakes within 0.2 magnitude units of the scenario event as this seismological characteristic has the greatest influence on the duration and frequency content of the record. The 25 selected records are chosen because they have a good match to the spectral shape of the 5%-damped target spectrum between 0.05 to 2.5s periods. This match is assessed using the RMS difference between the normalized spectral accelerations of the observed and target spectra (ΔSAn_{RMS}) based on the proposal of Ambraseys *et al.* (2004):

$$\Delta SAn_{RMS} = \sqrt{\frac{1}{N_p}\sum_{i=1}^{N_p}\left(\frac{PSA_0(T_i)}{PGA_0} - \frac{PSA_S(T_i)}{PGA_S}\right)^2} \qquad (3)$$

where N_p is the number of periods at which the spectral shape is specified, $PSA_0(T_i)$ is the pseudo spectral acceleration from the record at period T_i, $PSA_S(T_i)$ is the target pseudo spectral acceleration at the same period; PGA_0 and PGA_S are the peak ground acceleration of the accelerogram and the zero-period anchor point of the target spectrum. Selecting accelerograms on the basis of spectral shape is conducted to prevent the bias observed by Watson-Lamprey and Abrahamson (2006b) in the response of inelastic SDOF systems when linearly scaling accelerograms which consistently have a peak or trough at the initial period of the structure (Baker and Cornell 2006).

As indicated in Table 1, once the second set of 25 accelerograms were selected on the basis of magnitude and spectral shape, the various linear scaling (groups B1, B2, C1 and C2) or spectral matching (groups D1, D2, E1 and E2) techniques were applied to the records. These methods are briefly outlined below while specific details of the selected records may be obtained from Hancock (2006).

3.3 Linearly scaled to PSA at the initial period of the structure

Accelerograms in groups B1 and B2 are linearly scaled so that they match the median (group B1) and 84th-percentile (group B2) of the 5% damped target spectra at the initial period of the structure (0.56s). This scaling definition is based on that used by many other researchers (e.g., Shome *et al.*1998; Iervolino and Cornell 2005). As the records have been chosen based on spectral shape, the average spectra also have a reasonable match with the target spectra (Figure 5).

3.4 Linearly scaled average PSA

Groups C1 and C2 contain accelerograms scaled so that the median spectral acceleration matches the target spectral acceleration in the period range of relevance to this structure; from approximately twice the initial period, to account for stiffness degradation, to approximately half to account for higher mode effects (frequency analysis shows that the structure is first mode dominated and only the second mode has significant modal participation). Linear scaling of the records is conducted to minimize the RMS of the PSA for spectral ordinates at periods between 0.25s and 1.2s for all records, whilst ensuring the median spectral acceleration of the records at any point in this period range do not fall below 5% of the target spectrum (Figure 6).

3.5 Spectrally matched to 5% elastic spectrum using wavelet adjustments

Groups D1 and D2 consist of 25 spectrally matched accelerograms that have been adjusted with wavelets using RspMatch2005 (Hancock *et al*. 2006) to match the smooth 5%-damped elastic target response spectrum. Initially the accelerograms are linearly scaled on an individual basis in order to have a good match to the target spectrum. They are then adjusted using RspMatch2005 so that they match the 5% damped target spectrum over the period range 0.05s to 2.5s. The scaling and matching exercise is repeated to produce two suites of records: the first set to match the median spectral acceleration (group D1) and the second matching the 84th-percentile spectral acceleration, group D2 (Figure 7). Pseudo spectral acceleration is used in this work because it is directly related to spectral displacement, which thus ensures that the accelerograms simultaneously match both the acceleration and displacement spectra.

3.6 Spectrally matched to elastic spectra at multiple damping levels using wavelet adjustments

Groups E1 and E2 are adjusted using RspMatch2005 in order to simultaneously match the 1%, 5%, 10% and 20% damped response spectra (Figure 8). The median response of the accelerograms shows a good match to the target spectra. However, it is difficult to match the response at the 1% damping level and the standard deviation of the responses at this damping level is ±20% at 0.5s period, which compares with standard deviations of between ±2% to ±10% for the other damping levels. The scaling and matching exercise is again repeated to produce two suites of records: the first set to match the median spectral acceleration (group E1) and the second to match the 84th-percentile spectral acceleration, group E2 (Figure 8).

4. RESPONSE FROM SCALED AND MATCHED ACCELEROGRAMS

4.1 Theory

Different response measures are used to compare the response of the wall-frame structure under the action of records selected and scaled using different methods. The standard error of the estimate (*SEE*) is used to measure the level of confidence that can be attributed to a result obtained from a sample of data:

$$SEE = \frac{\sigma}{\sqrt{N_{\mathrm{obs}}}} \tag{4}$$

where σ is the standard deviation of the underlying random variable (assumed to be equivalent to the sample standard deviation for the purposes of the analysis) and N_{obs} is the number of observations (Benjamin and Cornell 1970). The assumption that the sample and population standard deviations are equal is technically not correct but it is an assumption that is very commonly made and is unlikely to have any significant practical effect on the calculated *SEE*. Equation (4) may be rearranged as in Equation (5) and then used to determine the number of records required to predict some measure of structural response to a certain accuracy, *SEE*, given the standard deviation of the response, σ:

$$N_{\mathrm{obs}} = \left(\frac{\sigma}{SEE}\right)^2 \tag{5}$$

However, this equation does not provide any information regarding whether or not the geometric mean of the sample is biased. A biased estimate is defined here as an estimate that does not agree with the expected response of the structure as obtained through the use of the prediction equations discussed in section 2.5. The very large number of records (1656) that were used in the development of these equations enables the expected response, and therefore the estimate of any bias, to be predicted with a reasonable level of confidence. That said, very few of the 1656 records that were used in the development of the model actually correspond to scenarios that are similar to that being considered herein and as such there will inevitably be a significant degree of epistemic uncertainty associated with the estimate of the 'true' response.

4.2 Number of accelerograms required to estimate inelastic response

The focus is now turned to the presentation of the key results regarding how many records are required to achieve an estimate of inelastic response to within a certain standard error. This study confirms the findings of earlier researchers (e.g., Shome *et al.* 1998) that the standard deviation of the response, and hence the number of records required to predict the response to a given level of confidence, is reduced through scaling the ground motions to the elastic spectral acceleration at the initial period of the structure (groups B1 and B2) when compared to using unscaled accelerograms selected purely on the basis of seismological characteristics (group A). However, this study also shows that further reduction in the number of required records may be achieved by scaling the accelerograms to match the target acceleration spectrum on average between periods of 0.25 and 1.2 seconds (groups C1 and C2). The number of records required to obtain an estimate of peak roof drift to within ±10% of the geometric mean of the 25 observations (as measured in logarithmic units) with a 64% confidence level (i.e., one standard deviation confidence) reduces by a factor of about 4 when records are scaled to the initial period of the structure instead of being unscaled. This reduces by a further factor of about 3 when records are selected and scaled to the average spectral acceleration over a range of periods (Table 2). This result is particularly useful as it reduces the number of records required to estimate measures of peak response (peak roof and interstorey drifts) to this confidence level from 13 unscaled records to a single record scaled to the average spectral acceleration. What is an even more significant result is that when the selected records are matched using RspMatch2005 to the target spectrum at a single damping ratio (Groups D1 and D2), or multiple damping ratios (Groups E1 and E2), the number of records required to predict the expected response for other damage measures, including end rotations and the Park and Ang damage index, also decreases significantly from the case where spectra are linearly scaled to the average spectral acceleration to just one or two records at the 64% confidence level. The quadratic nature of Equation (5) dictates that if one desired an estimate of the response to within ±5% of the sample median, the numbers of records that are required is roughly four times greater than for the ±10% case (in principle this relationship is exact, however, the term roughly is used as one will always work with whole numbers of records). This relationship means that as we consider a smaller confidence interval about the true (but unknown) median the reduction in the numbers of required records becomes more drastic as one considers more stringent scaling and matching approaches. When interpreting the results presented in Table 2 it is worth emphasising that if one conducts the stated number of time-history analyses using a given scaling or matching procedure, one is not guaranteed of observing a response within 10% of the true (unknown) median level. Rather, one should anticipate that 64% of the time this situation will arise.

The numbers of records required to estimate different local damage indices varies. Low-cycle fatigue and absorbed hysteretic energy have the greatest variability (Figure 3) and therefore require more records to predict the inelastic response to within a given confidence interval for a particular confidence level than measures of the peak response (Table 2). The absolute numbers of records required to predict the response is specific to the structure being considered; however, the trends in the reductions of the numbers of accelerograms required for the various damage measures and scaling and matching approaches are broadly consistent with previous studies and are therefore expected to be generally representative.

Table 2 also indicates that there are differences in the numbers of required records when one considers accelerograms scaled to different intensity levels. For example, there is a significant reduction in the numbers of records required to estimate the 84th percentile response level, in comparison with the median response level, for both low-cycle fatigue and hysteretic energy measures. For these response measures the reduction in the number of required records is attributed to the response being dominated by a few particularly strong inelastic cycles. Such large inelastic excursions tend to have less variability than the more frequent lower-amplitude cycles that govern the response from weaker ground-motions. For the other response measures, although it may be possible to infer some trends, it is most likely that the observed differences between the numbers of required records for the two considered intensity levels is a reflection of sampling uncertainty rather than any underlying physical cause.

5. ASSESSMENT OF BIAS

5.1 Bias of the geometric mean estimate

Although Equation (5) enables an estimate of the required number of accelerograms to be made, it does not provide any information as to whether or not the estimate of the inelastic response under these accelerograms will be biased. Figure 9 shows the observed inter-storey drifts for the first and sixth storey obtained from the suites of records scaled and matched according to the various methods outlined in this paper. These observations are compared directly with the expected values of the drifts at the median and 84th-percentile levels that are obtained from the predictive relationships presented in section 2.5. In general, the observed drifts match the median estimates of the predictive relationships very well over both storeys (similar agreement is observed for the other storeys not shown). The distributions of the responses appear to be lognormally distributed, as assumed in the regression models, with the exception of the responses due to the records in group A where the observed responses tend to have a weaker-than-expected clustering of observations about the median level. This apparent depart from lognormality is most likely due to the limitations that exist in terms of the numbers of available records rather than due to some underlying physical cause. The 84th-percentile results tend to match the predicted values very well at the lower storeys, storeys one and two, but are then systematically lower than the predicted values for the upper storeys for all of the proposed scaling and matching methods. It should be noted that although all of the adopted methods underestimate this level of response, accelerograms that are spectrally matched using RspMatch2005 are the least biased. However, it should also be noted that although the regression models are developed using a very large number of records, the number of records within this dataset corresponding to the design event of a magnitude 7, strike-slip earthquake, recorded at 5km distance may not fully represent the distribution of inelastic responses specified by the predictive models. For example, although the residuals are not observed to be biased *en masse* (Hancock 2006) the observations corresponding to records that match this design scenario may be slightly over-estimated by the predictive equations and this appears to be the case for some of the damage measures considered herein. The consequence is that the perceived bias may be partly associated with the particular scaling or matching procedure that is adopted but also partly due to an over-prediction of the expected value using the predictive equations for this scenario. This issue is unavoidable when estimating bias; the ‘true’ response level will always remain unknown. The approach taken in this study, to assume that the true response level may be estimated using the predictive equations derived from 1656 nonlinear time domain analyses must be considered as a very robust way of estimating the ‘true’ response. This reasoning is partly supported by the fact that the geometric means of the responses due to the various suites of records tends to match the median of the predictive equations very well. Therefore it is reasonable to assume that the main causes of the bias are the adopted scaling and matching approaches.

Figure 9 also shows the results for the local damage measures observed in an outer column in the first and sixth storeys. The agreement between the geometric means of the responses from the scaled and matched accelerograms with the estimates of the median and 84th-percentile values of the predictive equations for the local damage measures is not as strong as for the drifts. In this case it is likely that some of the perceived bias is a result of the difficulty associated with the development of predictive equations for these measures. In particular, the largest biases correspond to the hysteretic energy and the fatigue damage which were shown to be the most variable of the considered damage measures in Figure 3.

The key result shown in Figure 9 is that although each of the scaling and matching procedures adopted herein are able to adequately capture the expected response of the structure, the variability of the observations decreases consistently as one scales and matches the records using more stringent criteria, i.e., as one moves from linear scaling to the target acceleration at the initial period of the structure (Group B1) to spectrally matching to multiple damping ratios (Group E1). As has been seen previously, this variability has a direct influence upon the number of records that are required to obtain this estimate for a certain confidence interval and confidence level.

5.2 Scale Factor bias

The ability to linearly scale accelerograms without introducing bias (consistently over- or under-predicting the response with increasing scale factor) is checked by plotting the observed values of different damage measures against the scale factor used to scale the accelerogram (Figure 10). Linear trend lines are fitted through the data and show that there is no consistent increase or decrease of the response with the scale factor; indeed the coefficients of determination of the trend lines (R^2) are all less than 0.05. This shows that accelerograms can be scaled by a factor of 10 without causing a bias if they are initially selected to match the earthquake magnitude and spectral shape. This lack of bias also confirms the appropriateness of not imposing severe constraints on distance when searching for seed records for a given scenario (Bommer and Acevedo, 2004; Baker and Cornell, 2006). A bias might have been found if the records had not been initially selected to have a good match to the target spectrum. Such a bias would be consistent with the findings of previous studies such as Carballo (2000), Baker and Cornell (2006), Bazzurro and Luco (2006), and Watson-Lamprey and Abrahamson (2006b). All of the above studies identify the predominant source of the bias as being associated with the presence of records with peaks and troughs in their spectra. However, the initial selection on the basis of spectral shape that has been conducted in this study inhibits the selection of records that have a strong peak in their spectra at the initial period of the structure. Baker and Cornell (2006) state that “ε (or its implied effect on mean spectral shape) should be given primary consideration when selecting records”. This statement applies equally well to records with $\varepsilon=0$ as it does to positive epsilon values; the key to preventing bias is to ensure that the initial spectral shape is appropriate for the scenario in consideration. Most recently, Luco and Bazzurro (2007) have demonstrated that the bias in drift response introduced through linear scaling to the target spectral ordinate corresponding to the initial period of the structure is largely removed when records with spectral shape most similar to the target spectrum are considered. The explanation for the introduced bias is by now well-known; peaked records require lower-than-average scaling, but will cause less damage than records with relatively smooth spectral ordinates in the vicinity of the initial period of the structure. On the other hand, records with a trough at the initial period of the structure are likely to cause greater than expected damage (e.g., Baker and Cornell 2005; Watson-Lamprey and Abrahamson 2006b).

The fatigue and absorbed hysteretic energy damage measures are known to be dependent on ground-motion duration (e.g., Hancock and Bommer 2006). The lack of bias in these damage measures demonstrates that selecting records to match the earthquake magnitude is sufficient to prevent scale bias from different ground-motion durations. This lack of bias is even further ensured when the accelerograms are wavelet adjusted to match multiple damping ratios. Bommer and Mendis (2005) proved that damping correction factors, used to modify spectral ordinates derived from one damping ratio to another, are strongly dependent upon duration and this dependence has recently been taken into account by Cameron and Green (2007) and quantified by Stafford *et al.* (2008). If an accelerogram can be adjusted to match target spectra defined for multiple damping ratios simultaneously then the likelihood of properly capturing the duration of the scenario event is increased.

6. SUMMARY AND CONCLUSIONS

In an ideal world, once it was deemed appropriate to conduct an inelastic time-history analysis for a particular structure, the expected response for a given scenario earthquake would be obtained by analysing the response of the structure under the action of a very large number of real earthquake records that were consistent with this scenario. However, in reality this is not possible for two reasons: (1) there are usually not a large number of records that are consistent with a particular design scenario (although this is gradually changing over time), and (2) there is only so much time that can be devoted to running analyses in a design office environment and this is not something that is likely to change over time. For these reasons a compromise must be made. This compromise currently consists of using small numbers of linearly scaled or spectrally matched accelerograms in order to obtain an estimate of the response that would be obtained under the ideal scenario where no compromise was required. In this article it is demonstrated that spectrally matching accelerograms using wavelet adjustments offers an effective balance between the full rigour of the ideal case and the use of fully artificially spectrum-compatible records. The small sacrifice that must be made when using the wavelet approach is to make minor adjustments to the as-recorded accelerograms.

A thorough analysis of the effects of different linear scaling and spectral matching procedures has been presented using suites of records that have been selected according to state-of-practice approaches. Although more sophisticated selection procedures have been proposed in the literature on this subject, it is shown that relatively simple approaches are still very effective provided that adequate care is taken during the scaling and matching of the accelerograms. In particular, the key attributes of the records that should be accounted for during the selection procedure are the magnitude of the earthquake from which the record came and the shape of the response spectrum.

The analyses and results that are presented herein relate to a single structure exposed to records that are consistent with a single earthquake scenario. Although the results that are presented are very convincing, the possible limitations of this restricted analysis should be borne in mind when attempting to generalise these results for other structures and scenarios. Clearly, further research should be conducted to verify that the findings of this article also apply to alternative structures and scenarios. However, given that the scaling and matching procedures that have been adopted essentially evolve from each other in a fairly logical progression it would be surprising indeed if similar results were not obtained for alternative situations.

The method proposed herein to check for bias in the estimated response is shown to be effective, albeit time consuming. Such large numbers of analyses need not be considered for every structure, but they should at least be conducted for other structural models and earthquake scenarios in order to confirm that the results of this study may be generalised to other cases. The confidence that one places in the assessment of bias is closely related to the confidence that one places in the ability of the predictive equations to estimate the expected response. As these predictive models become better constrained, through the acquisition of more accelerograms, the proposed method for assessing bias will become even more robust.

The principal finding of this work is that the number of required records and the degree of bias both systematically decrease as one applies more constraint on the scaling and matching of accelerograms. Significant reductions in the required numbers of records may be achieved as one moves from: (1) linearly scaling records to match the target spectrum at the initial period of the structure; to (2) scaling records to match the target spectrum over a range of periods; to (3) spectrally matching the records to a single damping ratio using wavelet adjustments; and to (4) simultaneously matching records to target spectra defined for multiple damping ratios. The degree of bias that is found in all methods may be accounted for through the use of factors as commonly adopted elsewhere in design codes. However, the key result of this article is that the number of records that are required to obtain a robust estimate of the inelastic response may be significantly reduced through the use of the spectrally matched, wavelet adjusted, accelerograms.

ACKNOWLEDGEMENTS

We would like to thank Rui Pinho and Stelios Antoniou for assistance with the SeismoStruct program used in this work. We would also like to thank Norm Abrahamson and Jennie Watson-Lamprey for many interesting and fruitful discussions on this topic. The work of the first author is supported by a doctoral training grant from the EPSRC and a Marie Curie Fellowship and the third author is a fellow of the Willis Research Network.

REFERENCES

Ambraseys NN, Simpson KA, Bommer JJ. Prediction of horizontal response spectra in Europe. *Earthquake Engineering and Structural Dynamics* 1996; **25**(4): 371-400.

Ambraseys NN, Douglas J, Rinaldis D, Berge-Thierry C, Suhadolc P, Costa G, Sigbjörnsson R., Smit P. Dissemination of European strong-motion data, Vol. 2. *CD-ROM Collection* Engineering and Physical Sciences Research Council, United Kingdom, 2004.

Baker JW, Cornell AC. A vector-valued ground motion intensity measure consisting of spectral acceleration and epsilon. *Earthquake Engineering and Structural Dynamics* 2005; **34**: 1193-1217.

Baker JW, Cornell AC. Spectral shape, epsilon and record selection. *Earthquake Engineering and Structural Dynamics* 2006; **35**: 1077-1095.

Bazzurro P, Luco N. Do scaled and spectrum-matched near-source records produce biased nonlinear structural responses? *Eighth U.S. National Conference on Earthquake Engineering,* San Francisco, CA, 2006, paper 1029.

Benjamin JR, Cornell CA. *Probability, Statistics, and Decision for Civil Engineers*. McGraw-Hill, New York, 1970, 684p.

Beyer K, Bommer JJ. Relationships between median values and aleatory variabilities for different definitions of the horizontal component of motion. *Bulletin of the Seismological Society of America* 2006; **96**(4A): 1512-1522.

Bommer JJ, Ruggeri C. The specification of acceleration time-histories in seismic design codes. *European Earthquake Engineering* 2002; **16**(1): 3-17.

Bommer JJ, Acevedo AB. The use of real earthquake accelerograms as input to dynamic analysis. *Journal of Earthquake Engineering* 2004; **8**(S1): 43-91.

Bommer JJ, Mendis R. Scaling of spectral displacement ordinates with damping ratios. *Earthquake Engineering and Structural Dynamics* 2005; **34**: 145-165.

Boore DM, Joyner WB. Empirical prediction of strong ground motion. *Structural Engineering in Natural Hazards Mitigation: Proceedings of Papers Presented at the Structures Congress '93,* ASCE, New York, 1993; **1**: 241-246.

Cameron WI, Green RU. Damping correction factors for horizontal ground-motion response spectra. *Bulletin of the Seismological Society of America* 2007; **97**: 934-960.

Carballo JE. Probabilistic seismic demand analysis spectrum matching and design. *PhD Thesis* 2000, Stanford University, CA.

CEN Eurocode 8: Design of structures for Earthquake resistance-Part 1: General rules, seismic actions and rule for buildings. *EN 1998-1: 2004.* Comité Européen de Normalisation, Brussels, 2004.

Cornell CA, Jalayer F, Hamburger RO, Foutch DA. Probabilistic basis for 2000 SAC federal emergency management agency steel moment frame guidelines. *Journal of Structural Engineering* 2002; **128**(4): 526-533.

Douglas J. Earthquake ground motion estimation using strong-motion records: a review of equations for the estimation of peak ground acceleration and response spectral ordinates. *Earth Science Reviews* 2003; **61**(1-2): 43-104.

Hancock J. The influence of duration and the selection and scaling of accelerograms in engineering design and assessment. *PhD Thesis,* Imperial College London, United Kingdom, 2006, http://www3.imperial.ac.uk/geotechnics/publications/phdtheses.

Hancock J, Bommer JJ. Using spectral matched records to explore the influence of strong-motion duration on inelastic structural response. *Soil Dynamics and Earthquake Engineering* 2007; **27**(4): 291-299.

Hancock J, Watson-Lamprey J, Abrahamson NA, Bommer JJ, Markatis A, McCoy E, Mendis R. An improved method of matching response spectra of recorded earthquake ground motion using wavelets. *Journal of Earthquake Engineering* 2006; **10**(S1): 67-89.

IBC. International Building Code 2000 *International Code Council* ISBN 1892395258, 2000.

Iervolino I, Cornell AC. Record selection for nonlinear seismic analysis of structures. *Earthquake Spectra* 2005; **21**(3): 685-713.

Joyner WB, Boore DM. Peak horizontal acceleration and velocity from strong-motion records including records from the 1979 Imperial Valley, California, earthquake. *Bulletin of the Seismological Society of America* 1981; **71:** 2011-2038.

Joyner WB, Boore DM. Methods for regression analysis of strong-motion data. *Bulletin of the Seismological Society of America* 1993; **83**: 469-487.

Kircher CA. Code requirements for the selection and scaling of ground motion records. *Presentation made to the 2005 COSMOS Annual Meeting,* San Francisco, California, 2005.

Lee LH, Lee HH, Han SW. Method of selecting design earthquake ground motions for tall buildings. *Structural Design of Tall Buildings* 2000; **9**(3): 201-213.

Luco N, Bazzurro P. Does amplitude scaling of ground motion records result in biased nonlinear structural drift responses? *Earthquake Engineering and Structural Dynamics* 2007; **36**: 1813-1835.

McGuire RK. Probabilistic seismic hazard analysis and design earthquakes: Closing the loop. *Bulletin of the Seismological Society of America* 1995; **85**: 1275-1284.

Malhotra PK. Strong-motion records for site-specific analysis. *Earthquake Spectra* 2003; **3**: 557-578.

Mwafy A-A M. Seismic performance of code-designed RC buildings. *PhD Thesis,* Imperial College London, United Kingdom, 2001.

Naeim F, Lew M. On the use of design spectrum compatible time historeys. *Earthquake Spectra* 1995; **11**(1): 111-127.

Naeim F, Alimoradi A, Pezeshk S. Selection and scaling of ground motion time histories for structural design using genetic algorithms. *Earthquake Spectra* 2004; **20**(2): 413-426.

Park Y, Ang AH. Mechanistic seismic damage model for reinforced concrete. *Journal of Structural Engineering* 1985; **111**: 722-739.

PEER. PEER NGA Database. *Pacific Earthquake Engineering Research Center*, http://peer.berkeley.edu/nga/index.html, 2006

SeismoSoft. SeismoStruct - A computer program for static and dynamic nonlinear analysis of framed structures. *Online. Available from URL* http://www.seismosoft.com; 2005.

Shome N, Cornell AC, Bazzurro P, Carballo JE. Earthquakes, records and nonlinear responses. *Earthquake Spectra* 1998; **14**: 469-500.

Stafford PJ, Mendis R, Bommer JJ. The dependence of spectral damping ratios on duration and number of cycles. *Journal of Structural Engineering* 2008; *in press*.

UBC. Uniform building code 1994. *International Conference of Building Officials.* ISBN 1884590438; 1994.

Watson-Lamprey JA, Abrahamson NA. Selection of time series for analyses of response of buildings. *First European Conference on Earthquake Engineering and Seismology*, Geneva, Switzerland, 2006a, paper no. 248.

Watson-Lamprey JA, Abrahamson NA. Bias caused by use of spectrum compatible motions. *Eighth U.S. National Conference on Earthquake Engineering,* San Francisco, CA, 2006b, paper 0909.

Zhai C, Xie L. A new approach of selecting real input ground motions for seismic design: the most unfavourable real seismic design ground motions. *Earthquake Engineering and Structural Dynamics* 2007; **36**: 1009-1027.

Table 1. Different selection, scaling and matching methods used in this study

Group	**Selection Criteria**				**Linearly scaled or Spectrally Matched**	**Target**
	Mag.	**Dist.**	**Site**	**Spectral shape**		
A	√	√	√	X	None	None
B1	√	X	X	√	Linearly scaled	5% Damping, initial period PSA, median
B2	√	X	X	√	Linearly scaled	5% Damping, initial period PSA, 84th-percentile
C1	√	X	X	√	Linearly scaled	5% Damping, average PSA, median
C2	√	X	X	√	Linearly scaled	5% Damping average PSA, 84th-percentile
D1	√	X	X	√	Spectrally Matched	5% Damping, median
D2	√	X	X	√	Spectrally Matched	5% Damping, 84th-percentile
E1	√	X	X	√	Spectrally Matched	1, 5, 10 and 20% Damping, median
E2	√	X	X	√	Spectrally Matched	1, 5, 10 and 20% Damping, 84th-percentile

Table 2. Number of records required to predict different damage measures to within ±10% of the geometric mean of the sample (as measured in logarithmic units) with a confidence level of 64% using accelerograms selected, scaled and matched using different methods

Damage Measure	**Element / Location**	**Regression (unscaled)**	**Group**								
			A	**B1**	**B2**	**C1**	**C2**	**D1**	**D2**	**E1**	**E2**
Peak Drift	Roof	10	13	3	2	1	1	1	1	1	1
Peak Drift	1st Storey	11	17	6	4	2	3	2	1	1	1
End rotation	End 1st floor beam	5	11	3	3	1	3	1	1	1	1
	Base 1st floor column	10	22	6	6	3	4	2	1	1	1
Low-cycle fatigue	End 1st floor beam	133	161	36	15	20	10	19	5	9	4
	Base 1st floor column	152	167	82	54	44	34	28	6	14	5
Absorbed hysteretic energy	End 1st floor beam	17	43	31	34	29	18	31	5	25	4
	Base 1st floor column	110	138	54	5	15	3	11	3	5	2
Park and Ang damage index	End 1st floor beam	5	11	3	4	1	3	1	1	1	1
	Base 1st floor column	11	23	7	5	3	4	2	1	2	1

FIGURE CAPTIONS

Figure 1. Schematic illustration of the structural model adopted in this study (Mwafy 2001)

Figure 2. Magnitude-distance distribution of the dataset used in this study, identified by style-of-faulting and site classification.

Figure 3. Example median estimates of response for a selection of the predictive equations that have been developed for the structure considered in this study. The standard deviations of the models are also annotated on the plots. All predictions are shown for a strike-slip earthquake and for a site on soft soil and relate to the response of an outer first-storey column.

Figure 4. 5%-damped elastic response spectra for unscaled records selected on the basis of seismological characteristics (group A): *left* pseudo spectral acceleration, and *right* spectral displacement.

Figure 5. 5%-damped elastic spectral response from records scaled to the 5%-damped target spectral acceleration at the initial period of the structure. Records scaled to the median target spectra, group B1 (*upper*) and 84-percentile, group B2 (*lower*)

Figure 6. As Figure 5 but for records linearly scaled to match to the 5%-damped target spectral acceleration on average between 0.25 and 1.2s. Group C1 (*upper*), group C2 (*lower*).

Figure 7. 5% damped elastic spectral response from records matched to the 5%-damped target spectral acceleration using RspMatch2005. Records matched to the median target spectrum, group D1 (*upper*) and 84th-percentile, group D2 (*lower*)

Figure 8. Elastic response spectra adjusted using RspMatch2005 to simultaneously match the 1, 5, 10 and 20% damped target spectra. Records matched to the median target spectra, group E1 (*upper*) and 84th-percentile, group E2 (*lower*)

Figure 9. Damage measures from records selected and scaled using different methods. Error bars show median and ±1 standard deviation. Dashed lines show drift predicted by the regression equations derived from 1656 unscaled MDOF time-history analyses, long dashes correspond to the median while short dashes correspond to the 84th-percentile values.

Figure 10. Scale factor vs different response measures, demonstrating that there is no consistent increase or decrease (bias) introduced with the scale factor. Response from median level motions are plotted on the left while those from the 84th-percentile motions are plotted on the right. Straight lines show linear trend lines fitted through the data by least squares regression.

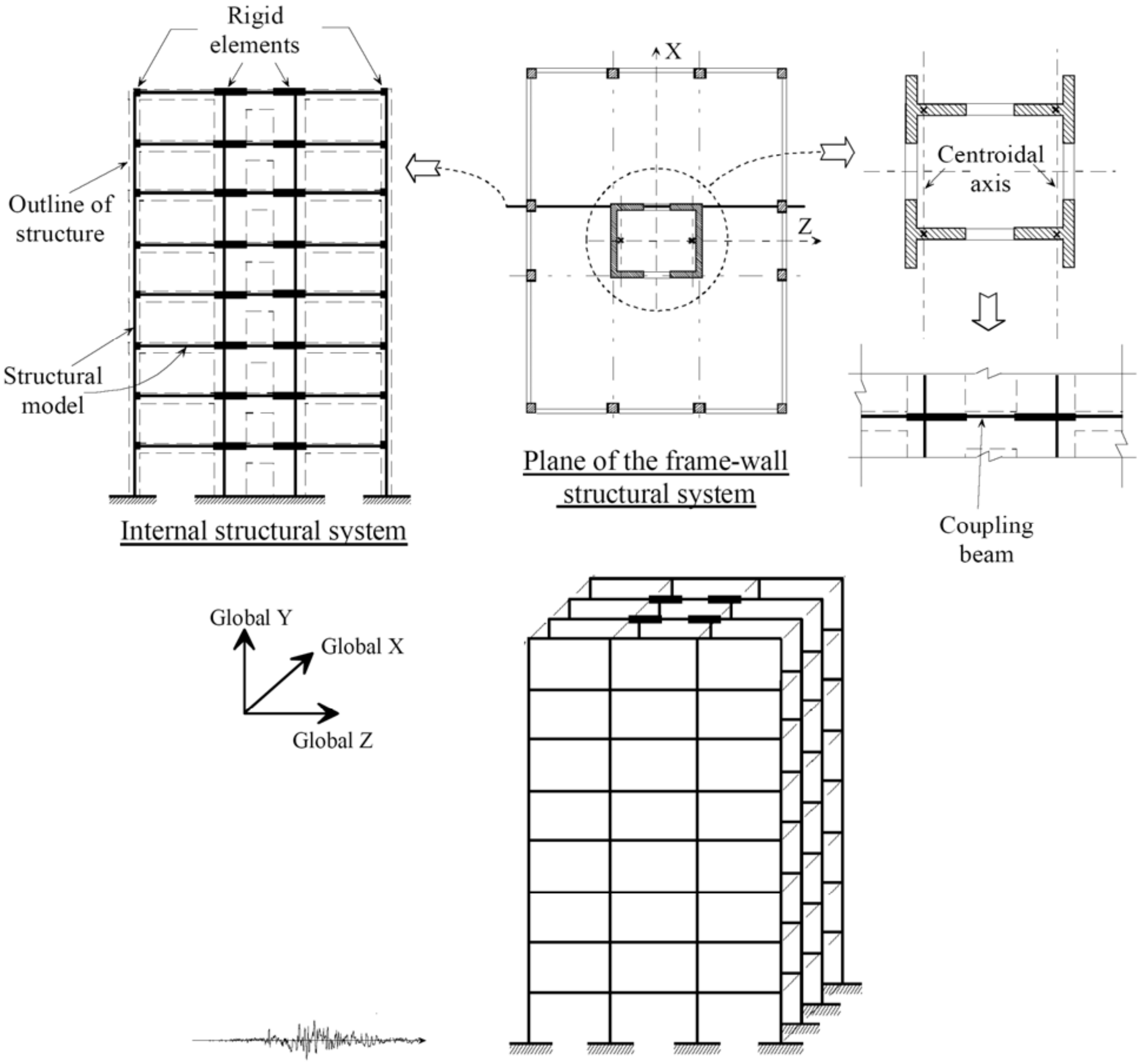
Rigid elements
Outline of structure
Structural model
Internal structural system
X
Z
Plane of the frame-wall structural system
Centroidal axis
Coupling beam
Global Y
Global X
Global Z

Figure 1

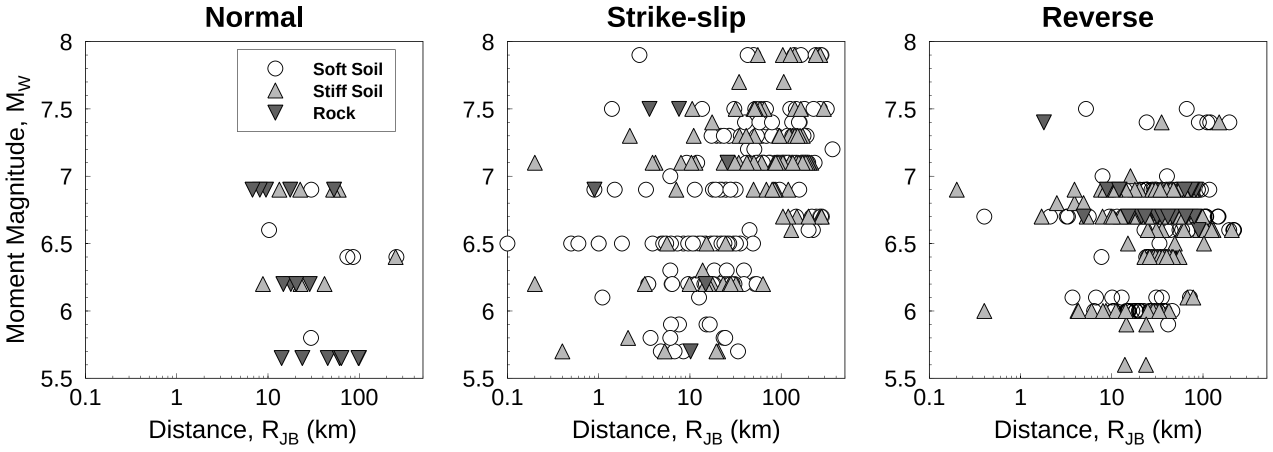
Normal
Strike-slip
Reverse
Moment Magnitude, M_W
Distance, R_{JB} (km)
Soft Soil
Stiff Soil
Rock
8
7.5
7
6.5
6
5.5
0.1
1
10
100

Figure 2

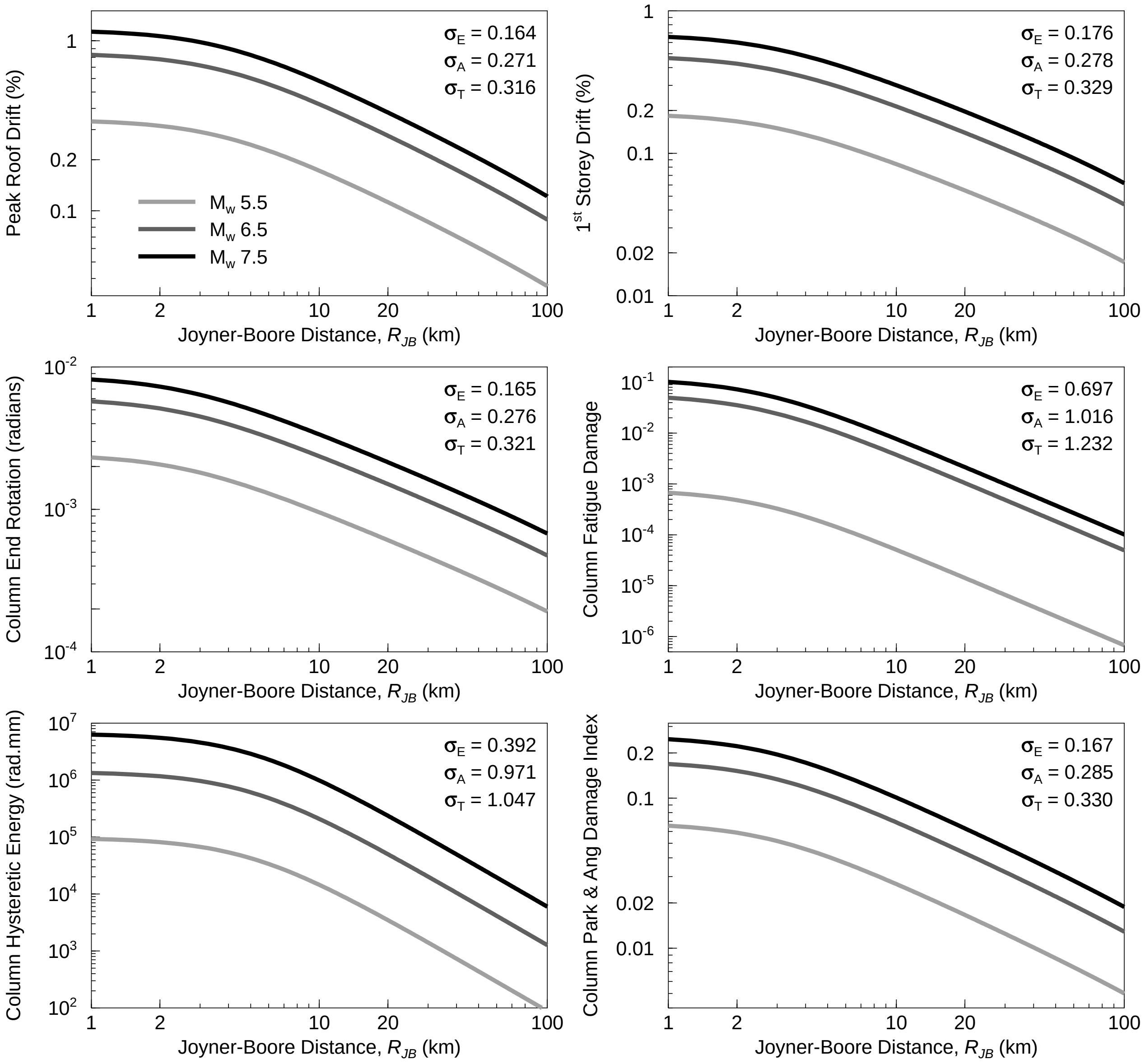
Peak Roof Drift (%)
σE = 0.164
σA = 0.271
σT = 0.316
Mw 5.5
Mw 6.5
Mw 7.5
1st Storey Drift (%)
σE = 0.176
σA = 0.278
σT = 0.329
Column End Rotation (radians)
σE = 0.165
σA = 0.276
σT = 0.321
Column Fatigue Damage
σE = 0.697
σA = 1.016
σT = 1.232
Column Hysteretic Energy (rad.mm)
σE = 0.392
σA = 0.971
σT = 1.047
Column Park & Ang Damage Index
σE = 0.167
σA = 0.285
σT = 0.330
Joyner-Boore Distance, RJB (km)
1
2
10
20
100

Figure 3

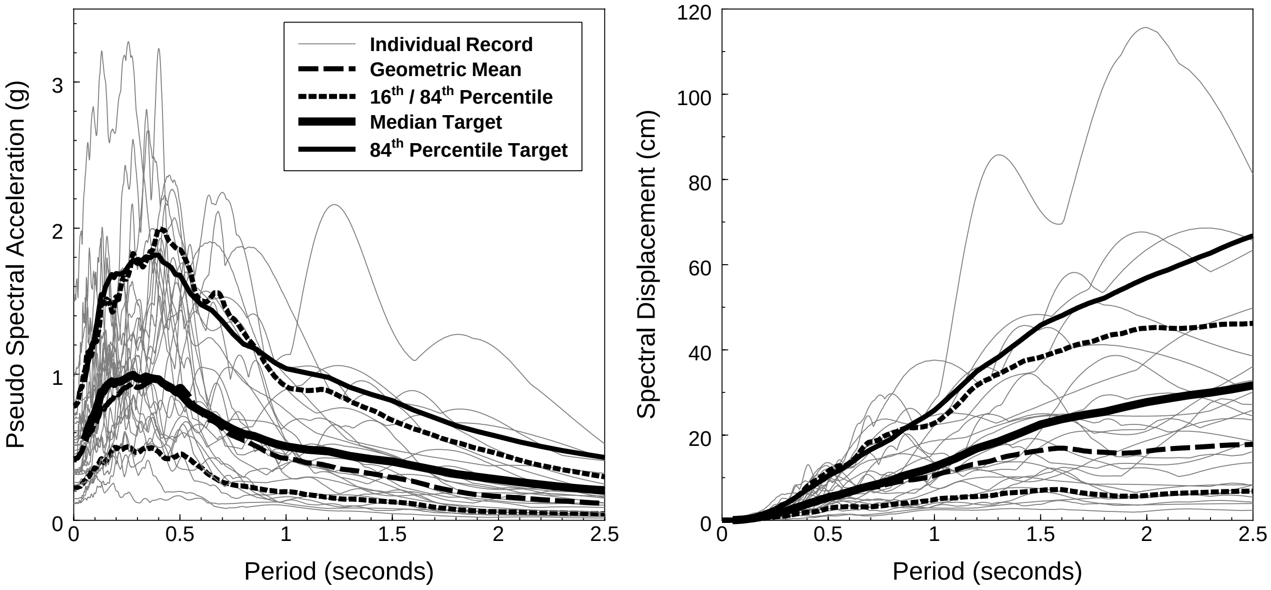
Individual Record
Geometric Mean
16th / 84th Percentile
Median Target
84th Percentile Target
Pseudo Spectral Acceleration (g)
0
1
2
3
0
0.5
1
1.5
2
2.5
Period (seconds)
Spectral Displacement (cm)
0
20
40
60
80
100
120
0
0.5
1
1.5
2
2.5
Period (seconds)

Figure 4

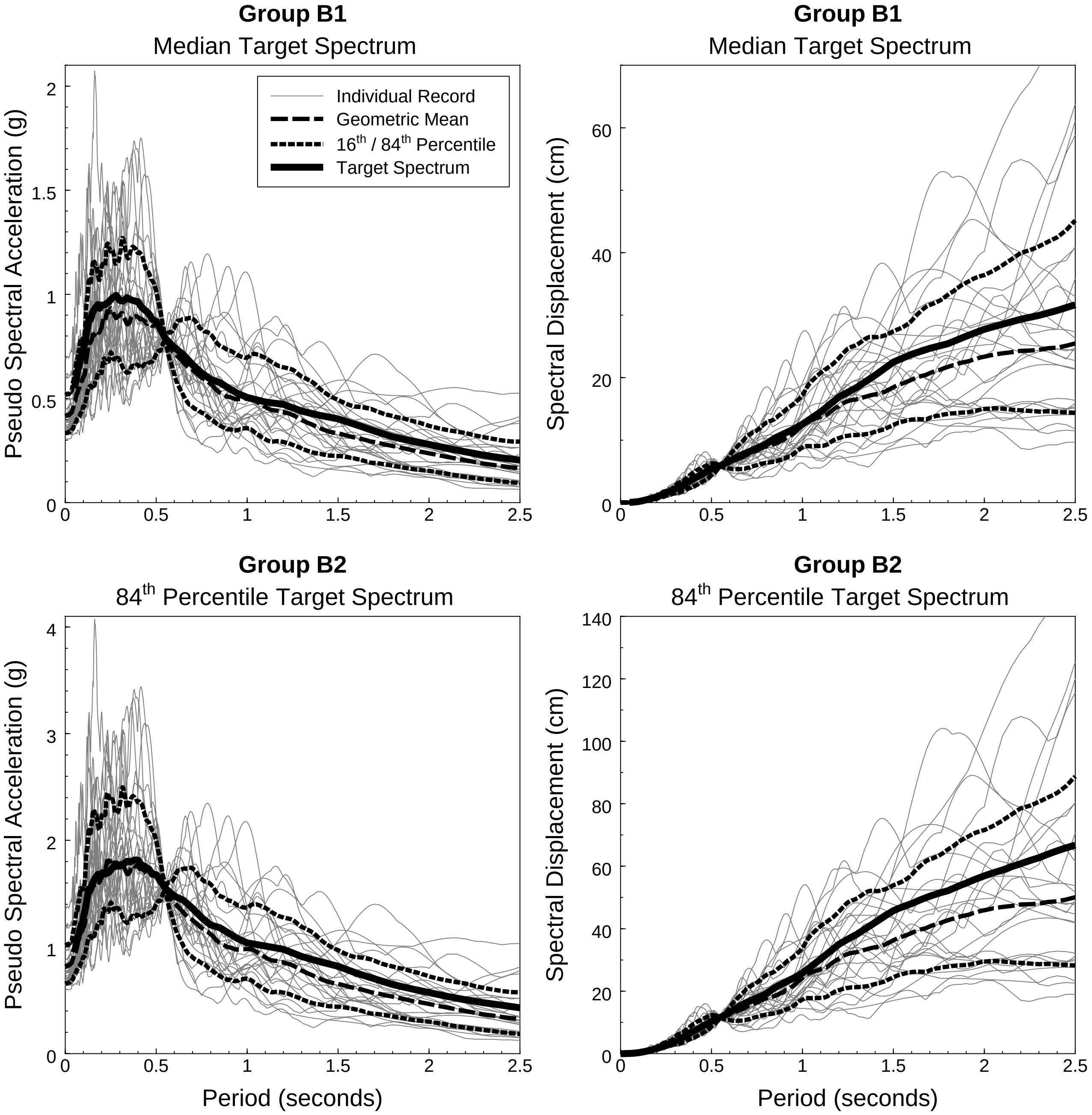
Group B1
Median Target Spectrum
Group B1
Median Target Spectrum
Group B2
84th Percentile Target Spectrum
Group B2
84th Percentile Target Spectrum
Individual Record
Geometric Mean
16th / 84th Percentile
Target Spectrum
Pseudo Spectral Acceleration (g)
Spectral Displacement (cm)
Period (seconds)
0
0.5
1
1.5
2
2.5
3
4
20
40
60
80
100
120
140

Figure 5

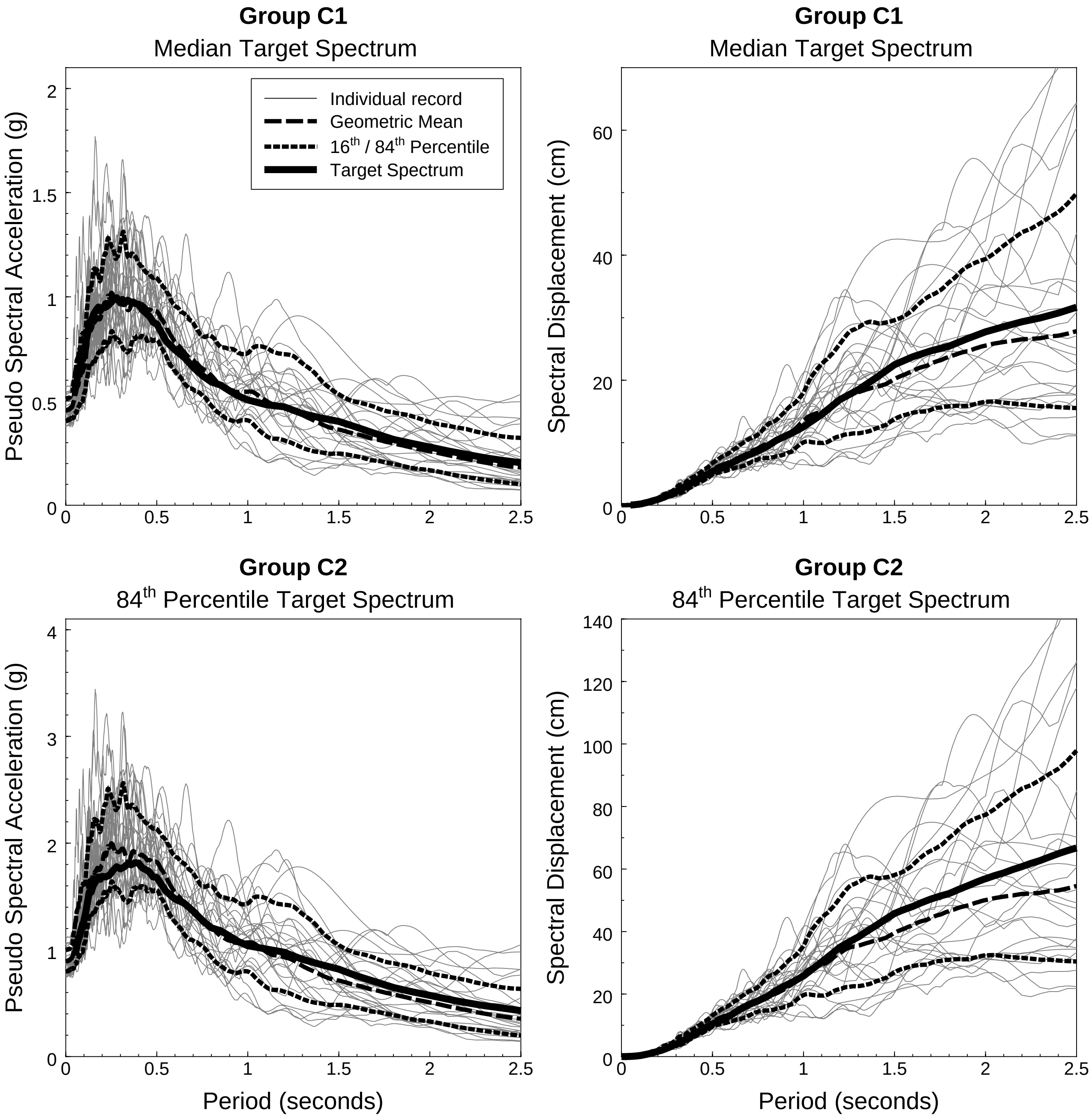
Group C1
Median Target Spectrum
Individual record
Geometric Mean
16th / 84th Percentile
Target Spectrum
Pseudo Spectral Acceleration (g)
0
0.5
1
1.5
2
0
0.5
1
1.5
2
2.5
Group C1
Median Target Spectrum
Spectral Displacement (cm)
0
20
40
60
0
0.5
1
1.5
2
2.5
Group C2
84th Percentile Target Spectrum
Pseudo Spectral Acceleration (g)
0
1
2
3
4
0
0.5
1
1.5
2
2.5
Period (seconds)
Group C2
84th Percentile Target Spectrum
Spectral Displacement (cm)
0
20
40
60
80
100
120
140
0
0.5
1
1.5
2
2.5
Period (seconds)

Figure 6

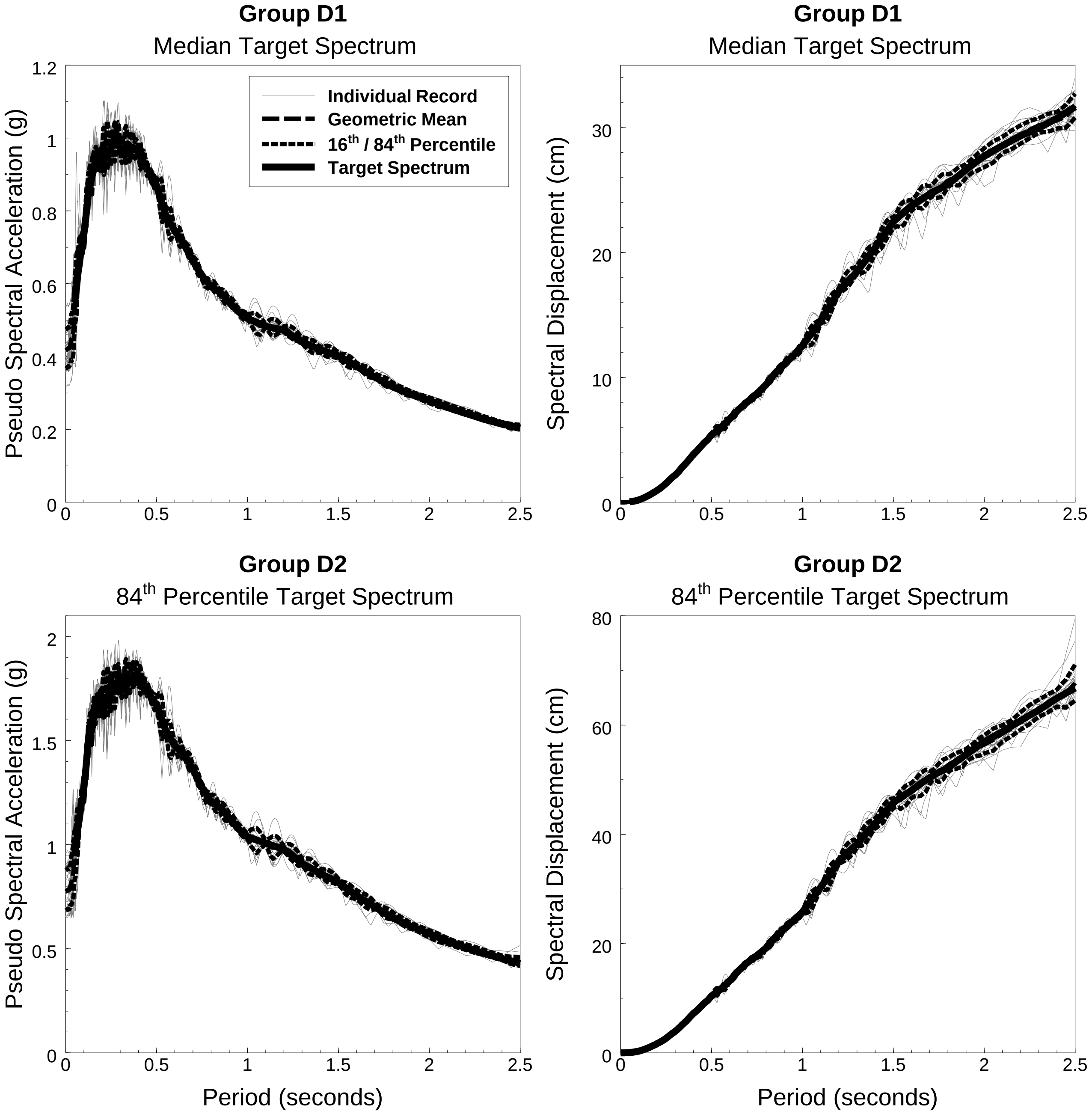
Group D1
Median Target Spectrum
Pseudo Spectral Acceleration (g)
Individual Record
Geometric Mean
16th / 84th Percentile
Target Spectrum
Spectral Displacement (cm)
Group D2
84th Percentile Target Spectrum
Period (seconds)
0
0.2
0.4
0.6
0.8
1
1.2
0.5
1.5
2
2.5
10
20
30
40
60
80

Figure 7

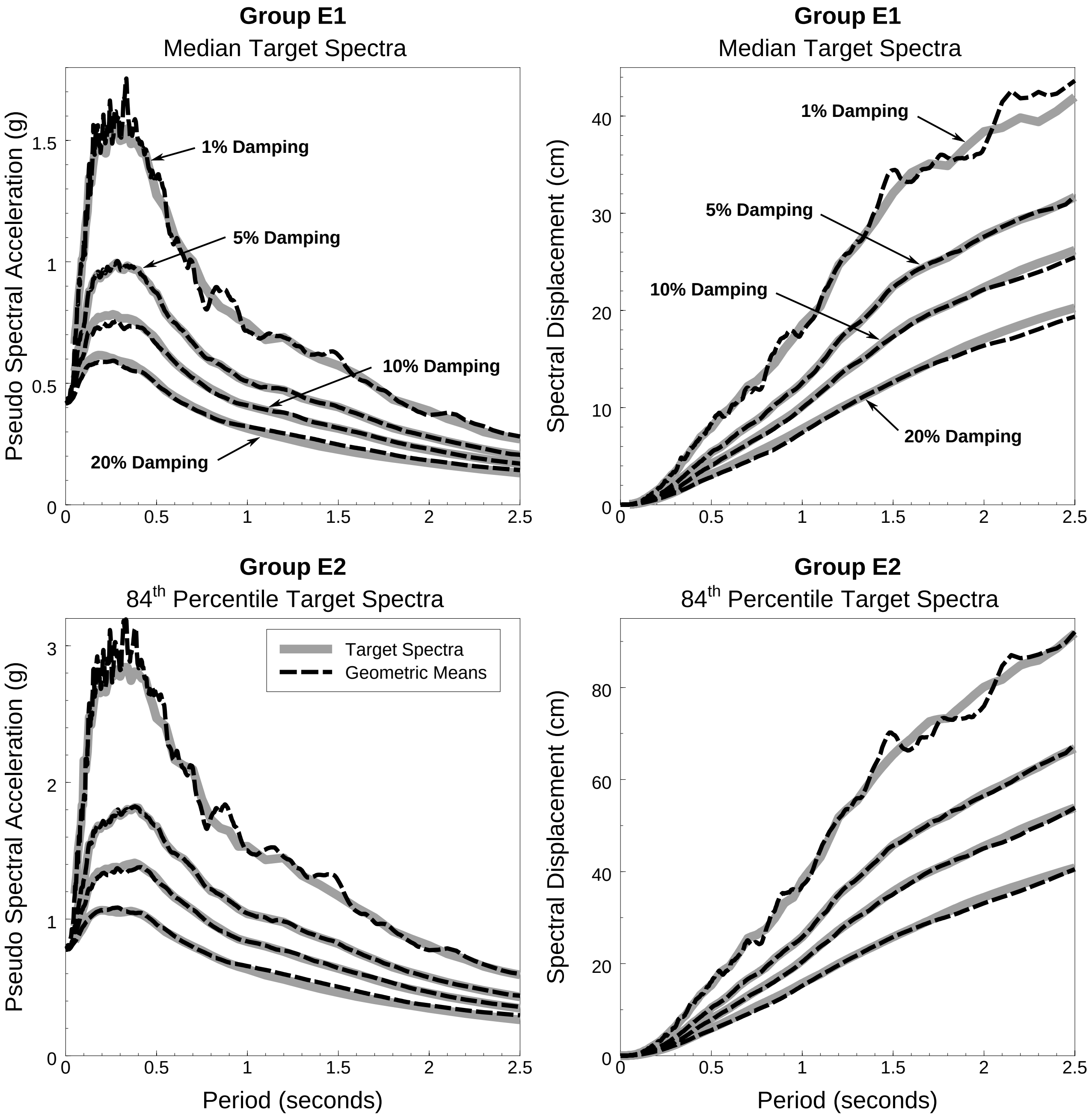
Group E1
Median Target Spectra
Pseudo Spectral Acceleration (g)
1% Damping
5% Damping
10% Damping
20% Damping
0
0.5
1
1.5
2
2.5
Group E1
Median Target Spectra
Spectral Displacement (cm)
1% Damping
5% Damping
10% Damping
20% Damping
0
10
20
30
40
Group E2
84th Percentile Target Spectra
Pseudo Spectral Acceleration (g)
Target Spectra
Geometric Means
0
1
2
3
Period (seconds)
Group E2
84th Percentile Target Spectra
Spectral Displacement (cm)
0
20
40
60
80
Period (seconds)

Figure 8

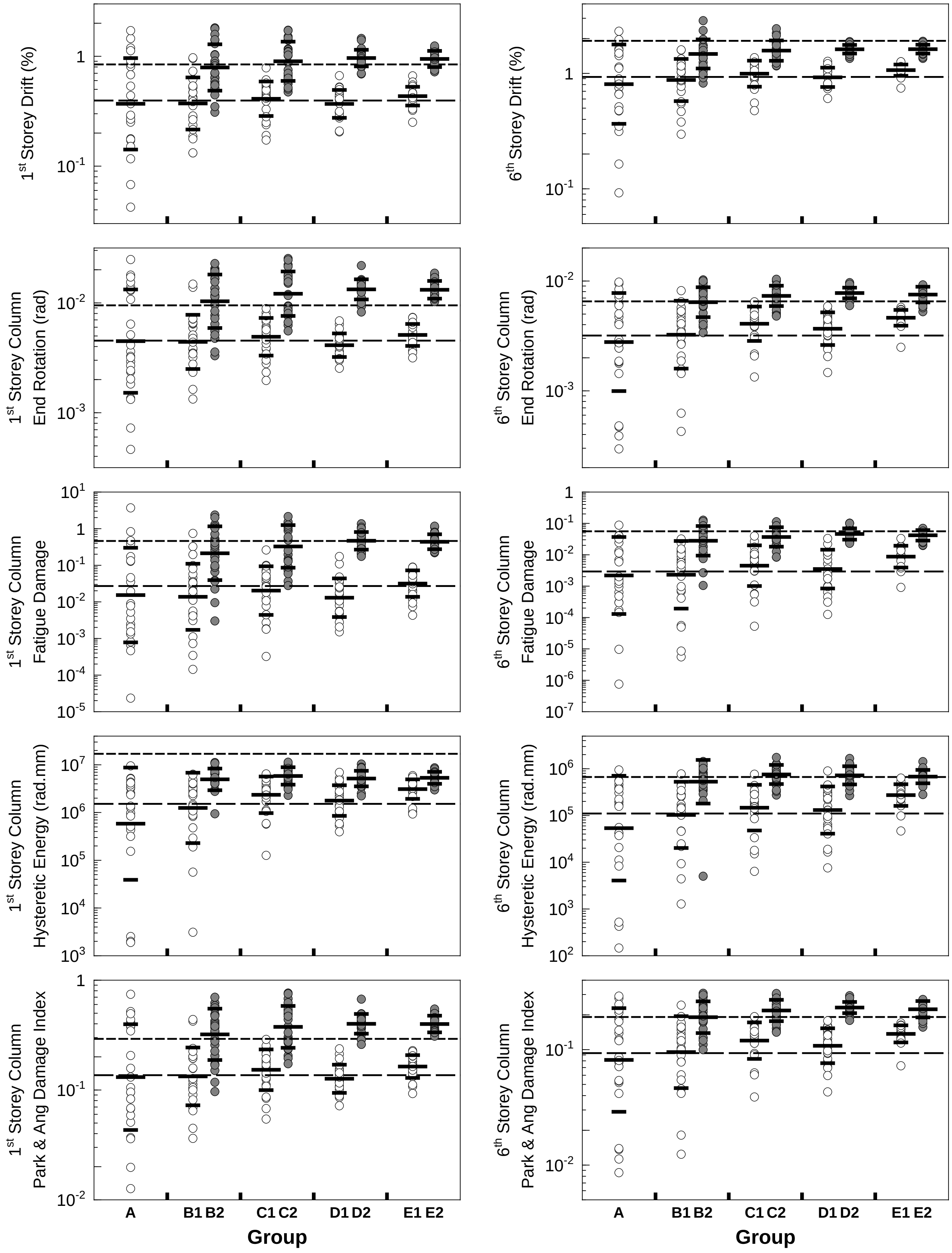

1st Storey Drift (%)
1
10-1
6th Storey Drift (%)
1
10-1
1st Storey Column End Rotation (rad)
10-2
10-3
6th Storey Column End Rotation (rad)
10-2
10-3
1st Storey Column Fatigue Damage
101
1
10-1
10-2
10-3
10-4
10-5
6th Storey Column Fatigue Damage
1
10-1
10-2
10-3
10-4
10-5
10-6
10-7
1st Storey Column Hysteretic Energy (rad.mm)
107
106
105
104
103
6th Storey Column Hysteretic Energy (rad.mm)
106
105
104
103
102
1st Storey Column Park & Ang Damage Index
1
10-1
10-2
6th Storey Column Park & Ang Damage Index
10-1
10-2
A
B1 B2
C1 C2
D1 D2
E1 E2
Group
A
B1 B2
C1 C2
D1 D2
E1 E2
Group

Figure 9

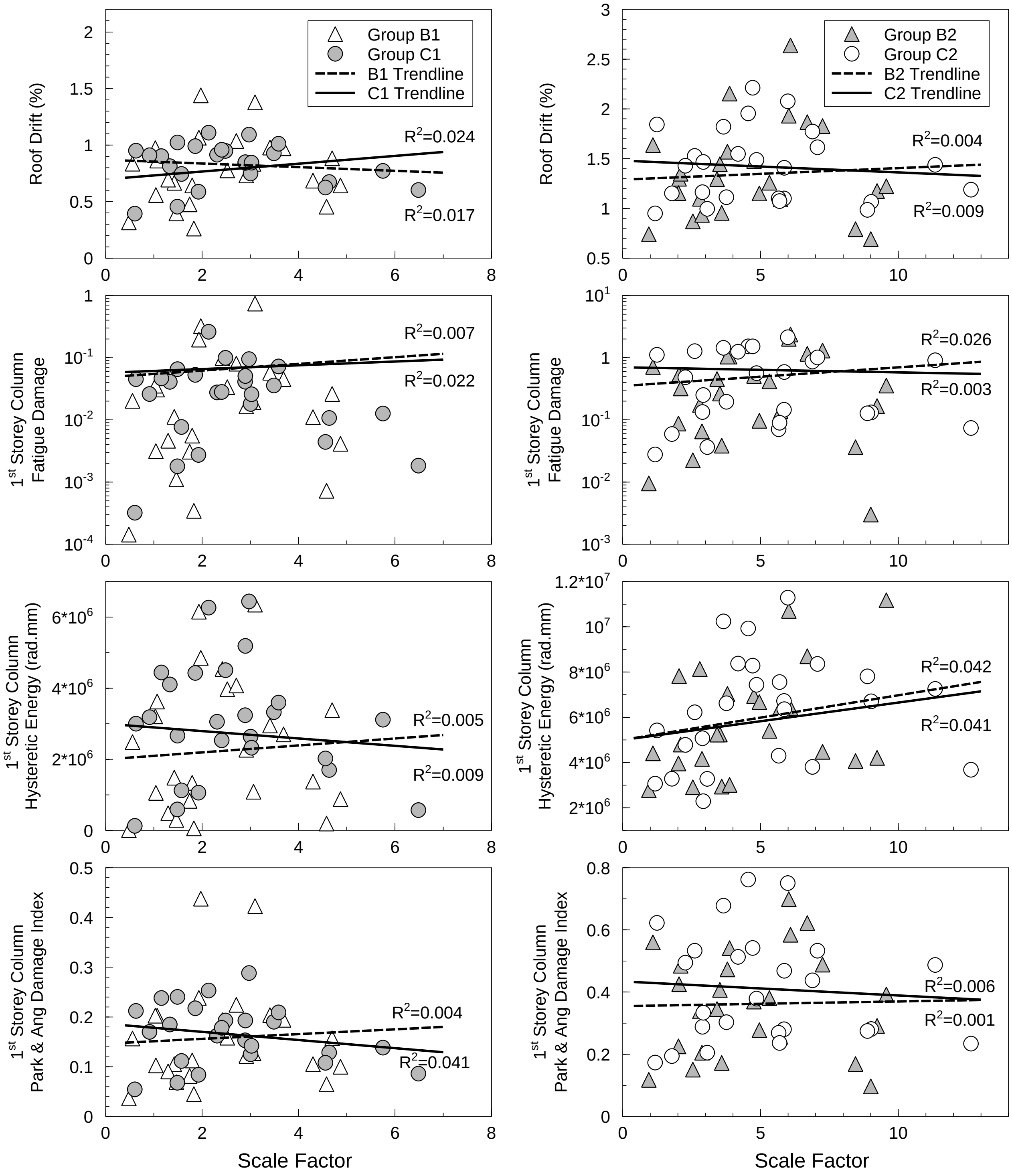
Group B1
Group C1
B1 Trendline
C1 Trendline
Group B2
Group C2
B2 Trendline
C2 Trendline
Roof Drift (%)
R^2=0.024
R^2=0.017
R^2=0.004
R^2=0.009
1st Storey Column Fatigue Damage
R^2=0.007
R^2=0.022
R^2=0.026
R^2=0.003
1st Storey Column Hysteretic Energy (rad.mm)
R^2=0.005
R^2=0.009
R^2=0.042
R^2=0.041
1st Storey Column Park & Ang Damage Index
R^2=0.004
R^2=0.041
R^2=0.006
R^2=0.001
Scale Factor
Scale Factor
0
2
4
6
8
0
5
10
0
0.5
1
1.5
2
0.5
1
1.5
2
2.5
3
10^{-4}
10^{-3}
10^{-2}
10^{-1}
1
10^{-3}
10^{-2}
10^{-1}
1
10^{1}
0
2*10^6
4*10^6
6*10^6
2*10^6
4*10^6
6*10^6
8*10^6
10^7
1.2*10^7
0
0.1
0.2
0.3
0.4
0.5
0
0.2
0.4
0.6
0.8

Figure 10